Supplemental Material Table 1. CLARS FTS Measurement Sequence

	Target Coordinate			Target Name	Measurement Mode
index	Latitude (degree)	Longitude (degree)	Altitude (meter)		
0	34.221	-118.057	1673	Spectralon®	SVO[1]
1	34.069	-117.390	340	Fontana	LABS[2]
2	34.081	-117.589	325	Rancho Cucamunga	LABS
3	33.951	-117.392	265	Riverside	LABS
4	33.877	-117.416	403	Lake Matt	LABS
5	33.962	-117.573	190	Norco	LABS
6	34.043	-117.725	253	Pomona	LABS
7	34.120	-117.868	217	210 Bend	LABS
8	33.868	-117.601	261	Corona	LABS
0	34.221	-118.057	1673	Spectralon®	SVO
9	33.863	-117.776	97	North OC	LABS
10	34.000	-117.883	151	60 Industry	LABS
11	34.110	-117.969	134	SantaFe Dam	LABS
12	33.678	-117.864	12	OC airPort	LABS
13	33.800	-117.883	47	Angels Stadium	LABS
0	34.221	-118.057	1673	Spectralon®	SVO
14	33.722	-117.975	12	Huntinghton beach	LABS
15	33.910	-118.006	57	La Mirada	LABS
16	34.030	-118.025	77	605 and 60	LABS
17	34.141	-118.042	155	Santa Anita Park	LABS
18	33.821	-118.195	11	Long Beach 405	LABS
19	33.930	-118.158	30	Downey	LABS
20	34.048	-118.116	128	ELA water	LABS
0	34.221	-118.057	1673	Spectralon®	SVO
21	33.810	-118.368	66	Palos Verdes	LABS
22	33.990	-118.400	8	Marina Del Rey	LABS
23	34.054	-118.305	58	Down Town Far	LABS
24	34.102	-118.234	124	Down Town Near	LABS
25	34.093	-118.470	257	Santa Monica	LABS
26	34.154	-118.273	160	Glendale	LABS
27	34.170	-118.165	293	west Pasadena	LABS
28	34.141	-118.353	170	Universal City	LABS

[1]Spectralon® Viewing Observations

[2]Los Angeles Basin Surveys

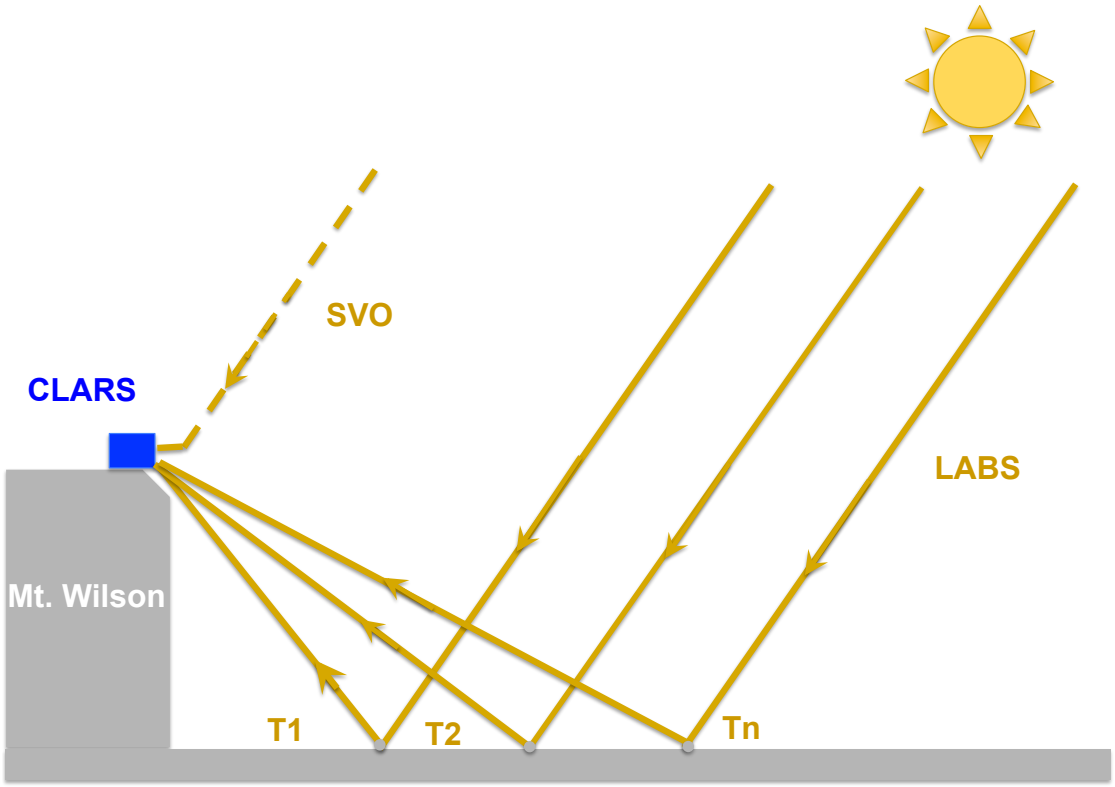

Los Angeles Basin

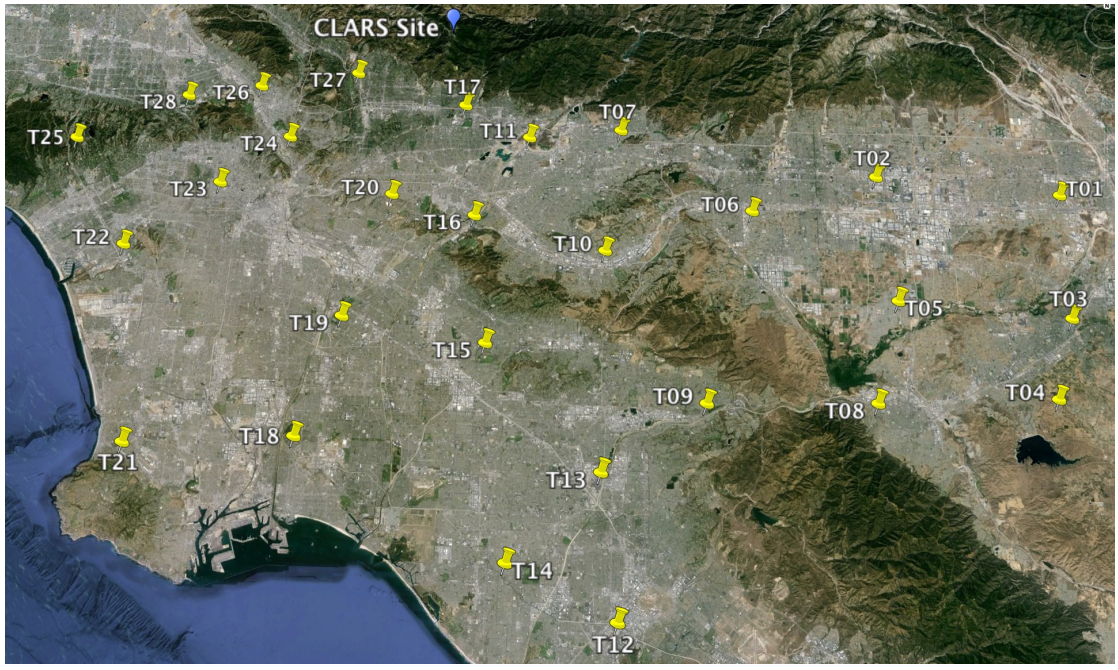

Supplemental Material Figure 1. Upper panel: Schematic diagram of spectrometer (altitude of 1.7 km) viewing geometry for Los Angeles Basin Surveys (LABS) and Spectralon® Viewing Observations; lower panel: the target site location of CLARS-FTS observations in a measurement sequence over Los Angeles Basin. Blue balloon indicates CLARS site; Yellow pins showed the target site location. The measurement sequence is being repeated daily for ~5-8 times. The sequences can be changed to accommodate the needs of special observations.

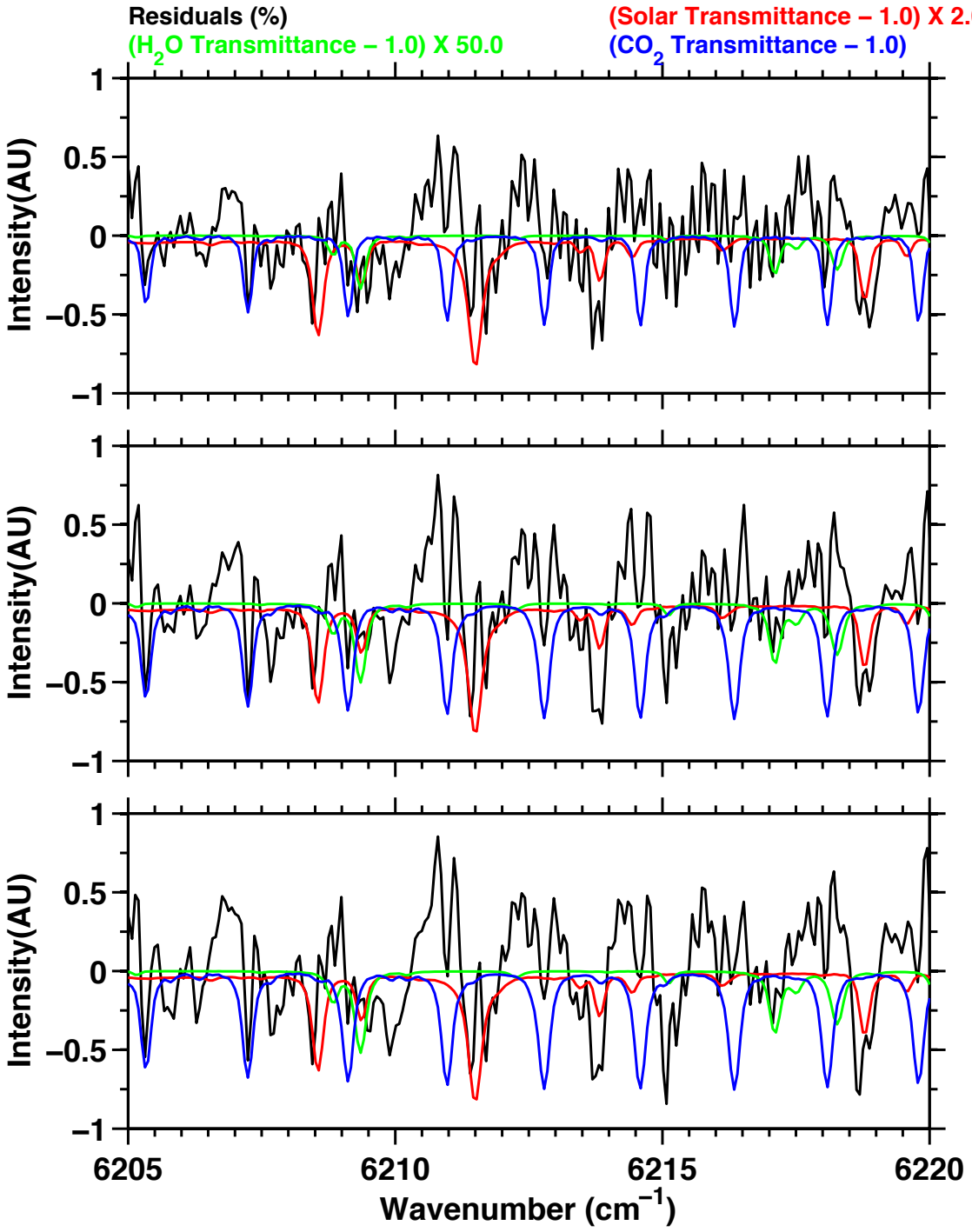

Supplemental Material Figure 2. Zoom-in view of MW6220 spectral fitting residuals (black curve) and scaled transmittances of solar spectrum (red curve), major interfering trace gases (green curve: H_2O spectral features), and CO_2 spectral features (blue curve) within the spectral segments. (top panels) for the measurements over CLARS site; (middle panels) for the measurements along the light path of pointing at the Santa Anita Race Track; and (bottom panels) for the measurements along the light path of pointing at the west Pasadena.

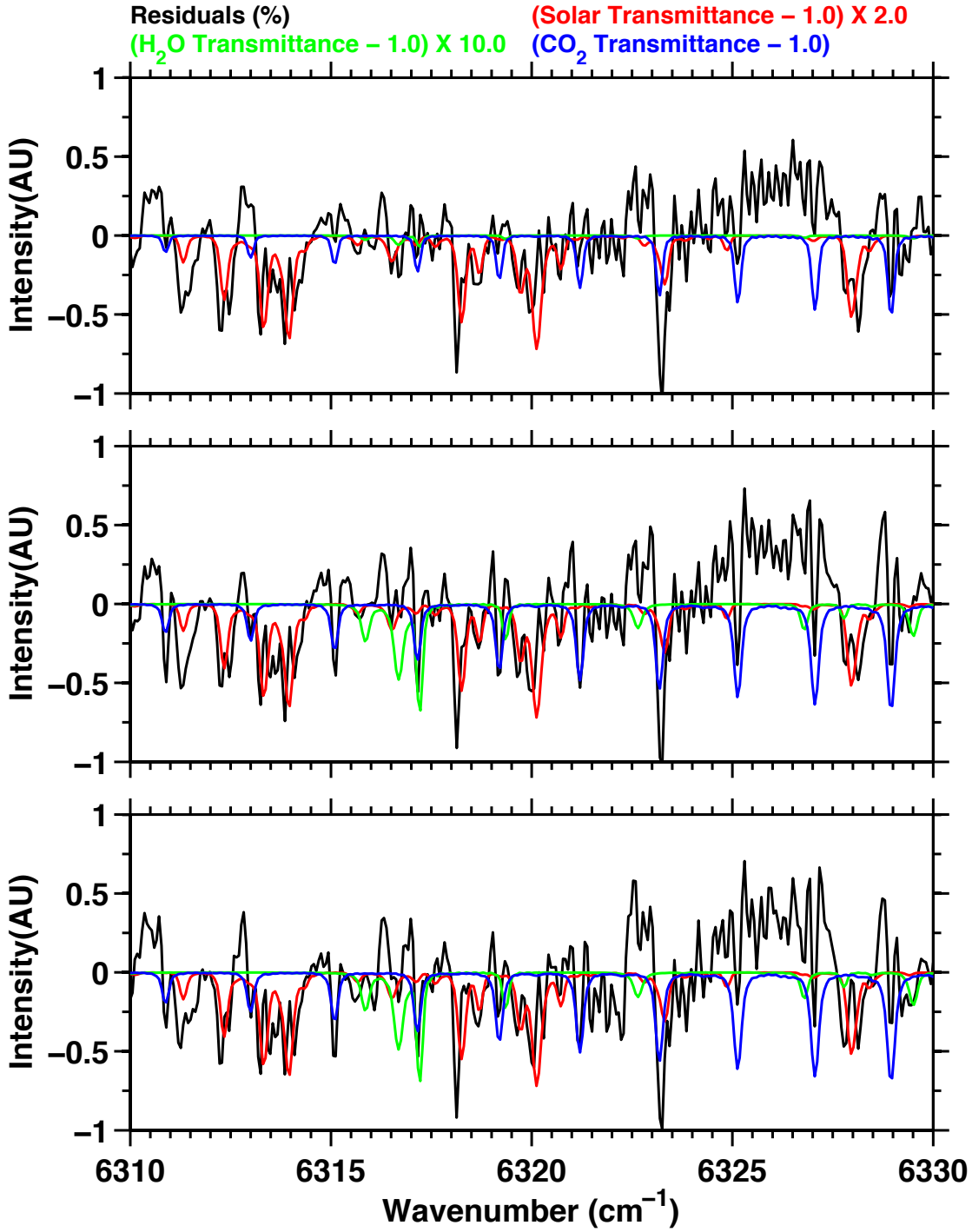

Supplemental Material Figure 3. Zoom-in view of MW6339 spectral fitting residuals (black curve) and scaled transmittances of solar spectrum (red curve), major interfering trace gases (green curve: H_2O spectral features), and CO_2 spectral features (blue curve) within the spectral segments. (top panels) for the measurements over CLARS site; (middle panels) for the measurements along the light path of pointing at the Santa Anita Race Track; and (bottom panels) for the measurements along the light path of pointing at the west Pasadena.

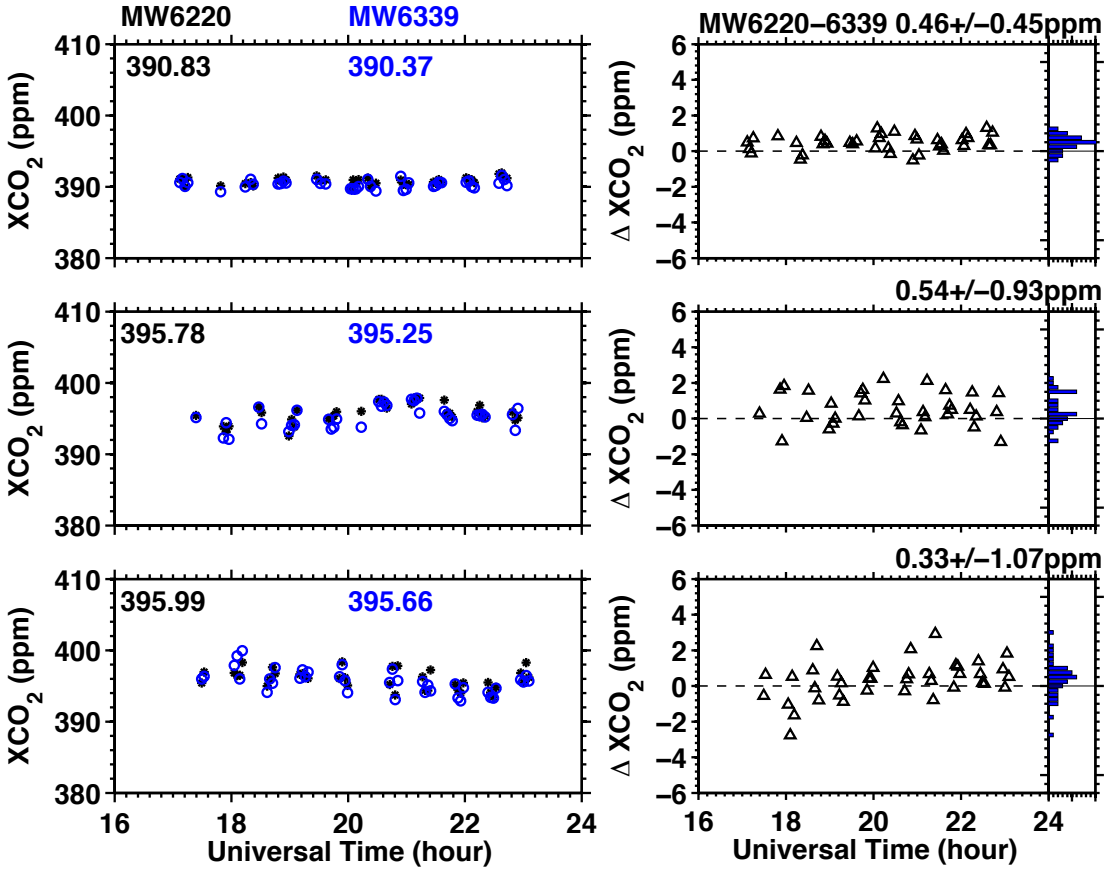

Supplemental Material Figure 4. XCO_2 (in parts per million (ppm)) measured by CLARS-FTS with MW6220 (black dots) and MW6339 (blue circles) on January 18th, 2013 (left panels) and differences of retrieved XCO_2 between the two spectral regions and the histograms (right panels) in the Spectralon® viewing geometry (top panels), towards the Arcadia Race Track (middle panels); and towards west Pasadena (bottom panels). Black stars in left panels: XCO_2 obtained using the spectral region of MW6220. Compared to the background levels of XCO_2 (top panels), XCO_2 over Arcadia Race Track (middle panels) and west Pasadena (bottom panels) show higher values (mean ART-SV: 4.91 ppm; mean WP-SV: 5.23 ppm) and present stronger diurnal cycles than those measurements over CLARS site. The XCO_2 values retrieved from MW6220 are higher than those of MW6339. The mean differences between MW6220 and MW6339 are 0.46 ppm, 0.54 ppm, and 0.33 ppm for SV, ART and WP measurements respectively. It was also appeared in the spectral analyses of the TCCON measurements (~0.15 ppm). Both CLARS-FTS and TCCON results, which are using HITRAN 2008 line list, show improvements on the band-to-band consistency of XCO_2, compared to those of using HITRAN 2004 line list such as Figure 6 of Washenfelder et al. (2006) with the XCO_2 using MW6220 about 0.9 ppm higher than that of MW6339. These systematic differences of retrieved XCO_2 values between two spectral bands are likely arisen from the discrepancies of spectroscopic parameters between two spectral bands and the amount/intensity of spectral features of interfering species.

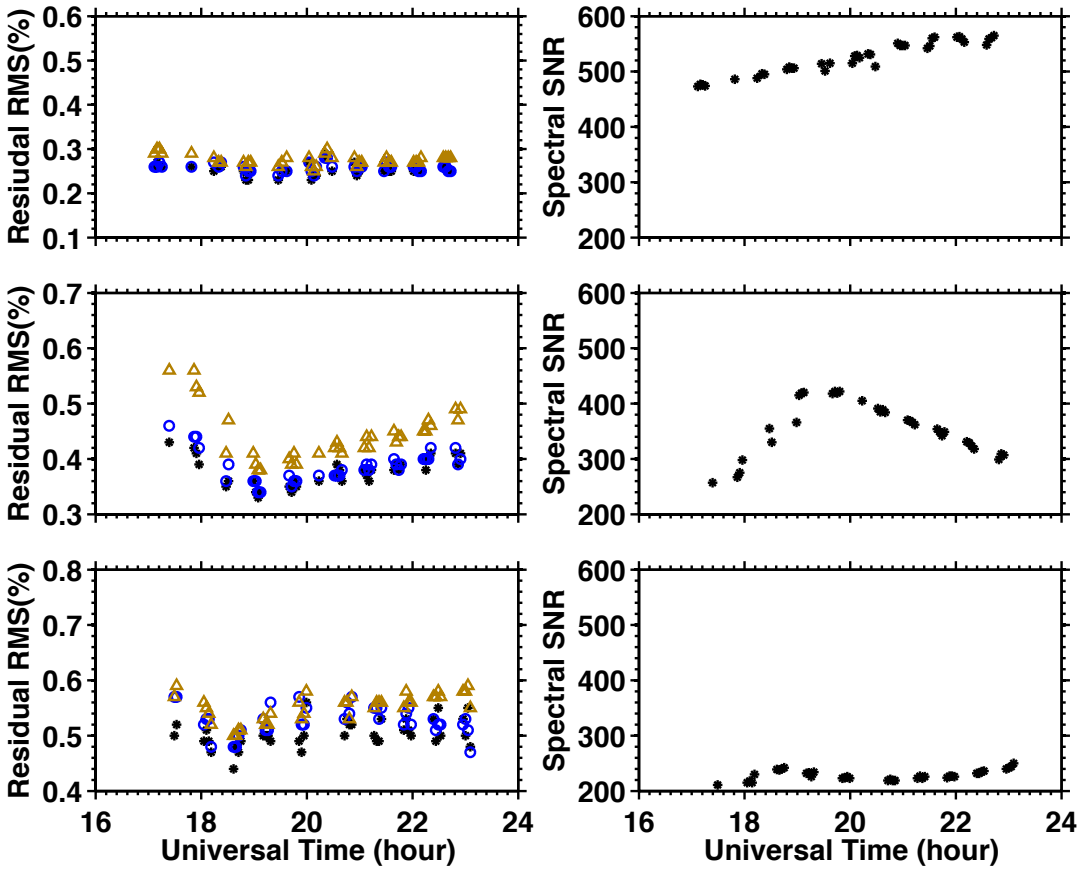

Supplemental Material Figure 5. Root Mean Square (RMS) of spectral fitting residuals (Left panels) and spectral SNR (Right panels) for CO_2 slant column density measurements as a function of time in Spectralon® viewing geometry (Top panels); over the Arcadia Race Track (Middle panels); over west Pasadena (Bottom panels). Three spectral bands centered at 6220 cm^{-1} (black stars, noted as MW6220 thereafter), 6339 cm^{-1} (blue circles, noted as MW6339 thereafter) and 7885 cm^{-1} (gold triangles, noted as MW7885 thereafter) are presented, respectively. The spectral SNR were nearly identical over the three spectral bands. The measurements were performed on January 18th, 2013. The spectral fitting residuals were normalized by the spectral continuum levels prior to the computation of RMS values. The spectral fitting residuals were dominated by the photon shot noise. The RMS of the spectral fitting residuals in both CO_2 bands are reasonably close to the expected values. The Chi-squared tests of spectral fitting residuals yielded values generally within 1.3.

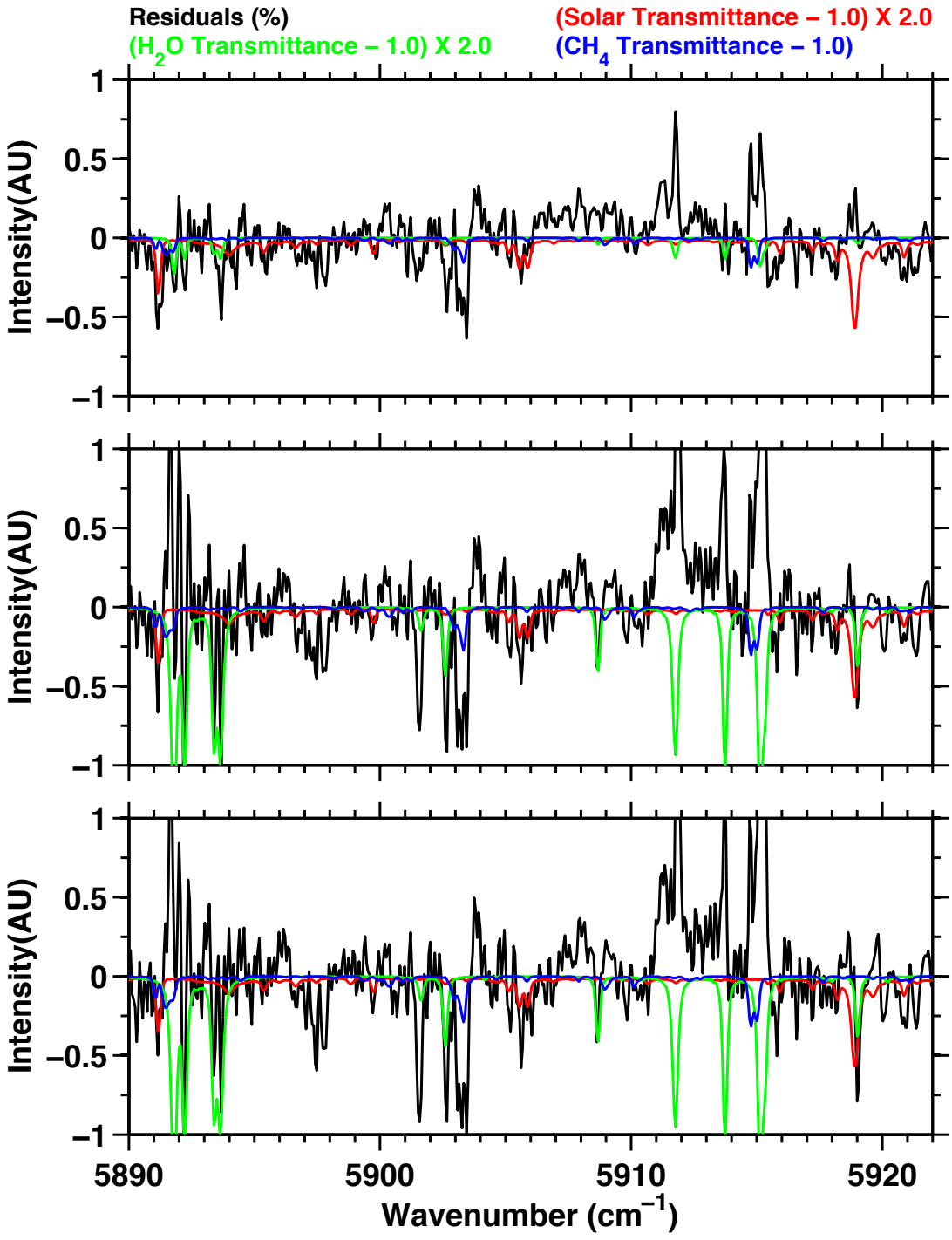

Supplemental Material Figure 6. Zoom-in view of MW5938 spectral fitting residuals (black curve) and scaled transmittances of solar spectrum (red curve), major interfering trace gases (green curve: H_2O spectral features), and CH_4 spectral features (blue curve) within the spectral segments. (Top panels) for the measurements over CLARS site; (middle panels) for the measurements along the light path of pointing at the Santa Anita Race Track; and (bottom panels) for the measurements along the light path of pointing at the west Pasadena.

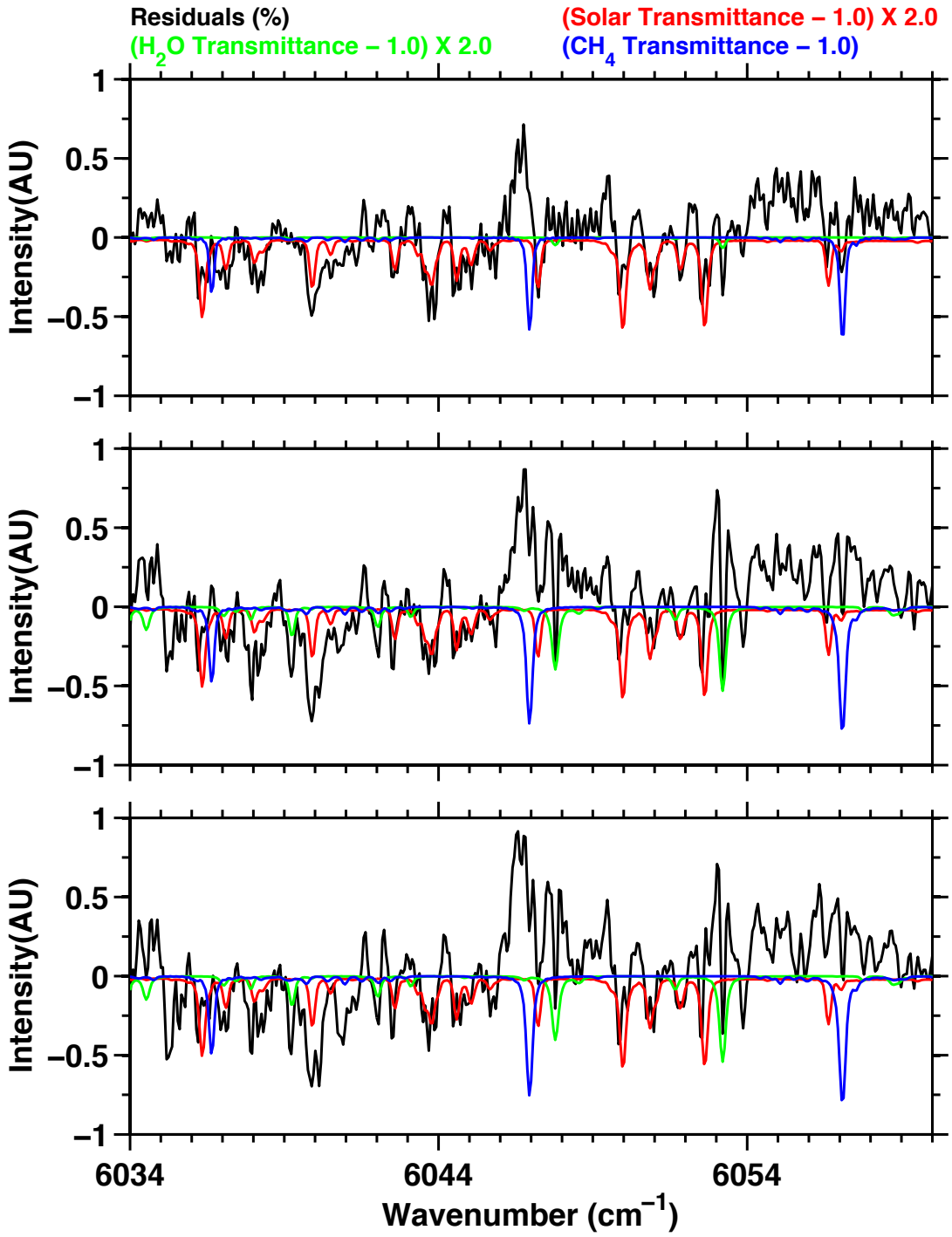

Supplemental Material Figure 7. Zoom-in view of MW6076 spectral fitting residuals (black curve) and scaled transmittances of solar spectrum (red curve), major interfering trace gases (green curve: H_2O spectral features)), and CH_4 spectral features (blue curve) within the spectral segments. (Top panels) for the measurements over CLARS site; (middle panels) for the measurements along the light path of pointing at the Santa Anita Race Track; and (bottom panels) for the measurements along the light path of pointing at the west Pasadena.

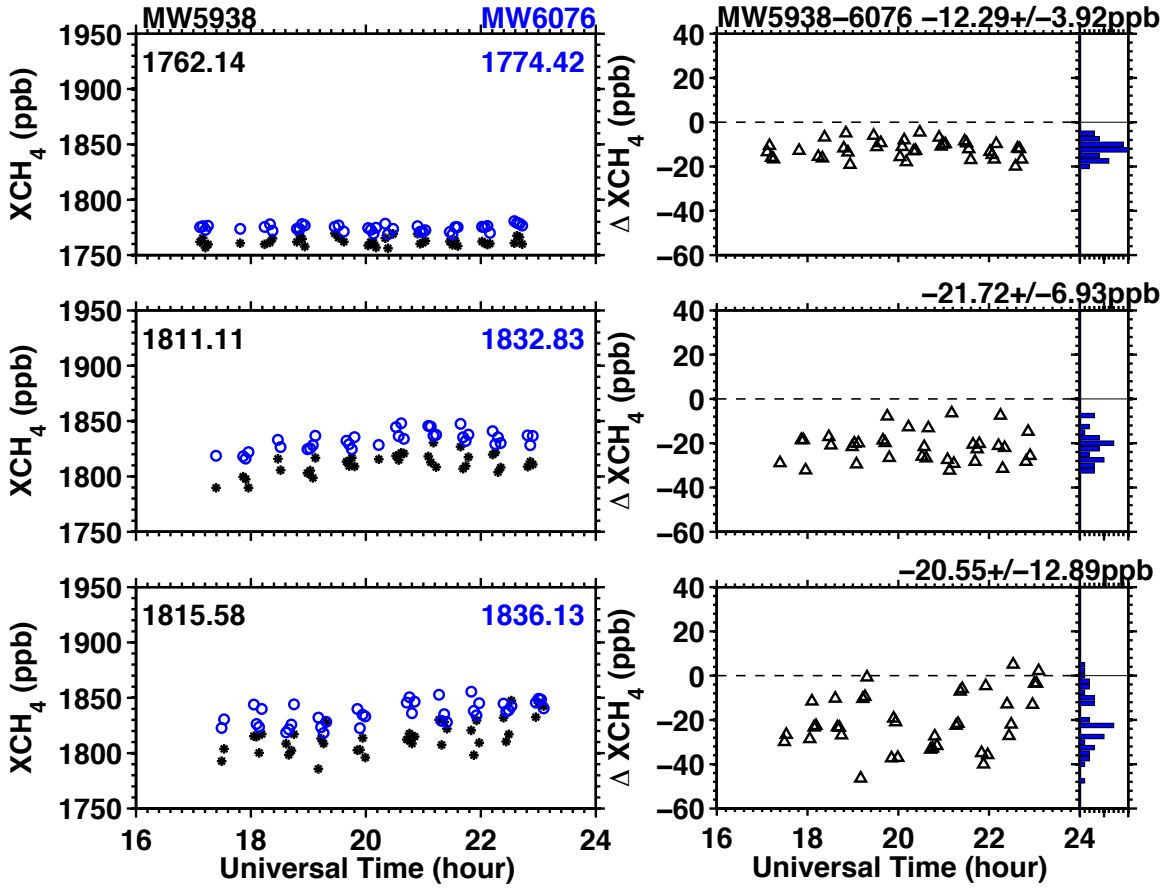

Supplemental Material Figure 8. XCH_4 (in parts per billion (ppb)) measured by CLARS-FTS with MW5938 (black dots) and MW6076 (blue circles) on January 18th, 2013 (left panels) and differences of retrieved XCH_4 between the two spectral regions and the histograms (right panels) in the Spectralon® Viewing geometry (top panels), towards the Arcadia Race Track (middle panels); and towards west Pasadena (bottom panels). Black stars in left panels: XCH_4 obtained using the spectral region of MW5938. Compared to the background levels of XCH_4 (top panels), XCH_4 over Arcadia Race Track (middle panels) and west Pasadena (bottom panels) show higher values (mean ART-SV: 53.69 ppb; mean WP-SV: 57.58 ppb) and present stronger diurnal cycles than those measurements over CLARS site. The XCH_4 values retrieved from MW6076 are higher than those of MW5938. The mean differences between MW6076 and MW5938 are 12.29 ppb, 21.72 ppb, and 20.55 ppb for SV, ART and WP respectively. These systematic differences of retrieved XCH_4 values between two spectral bands are likely arisen from the discrepancies of spectroscopic parameters between two spectral bands and the amount/intensity of spectral features of interfering species.

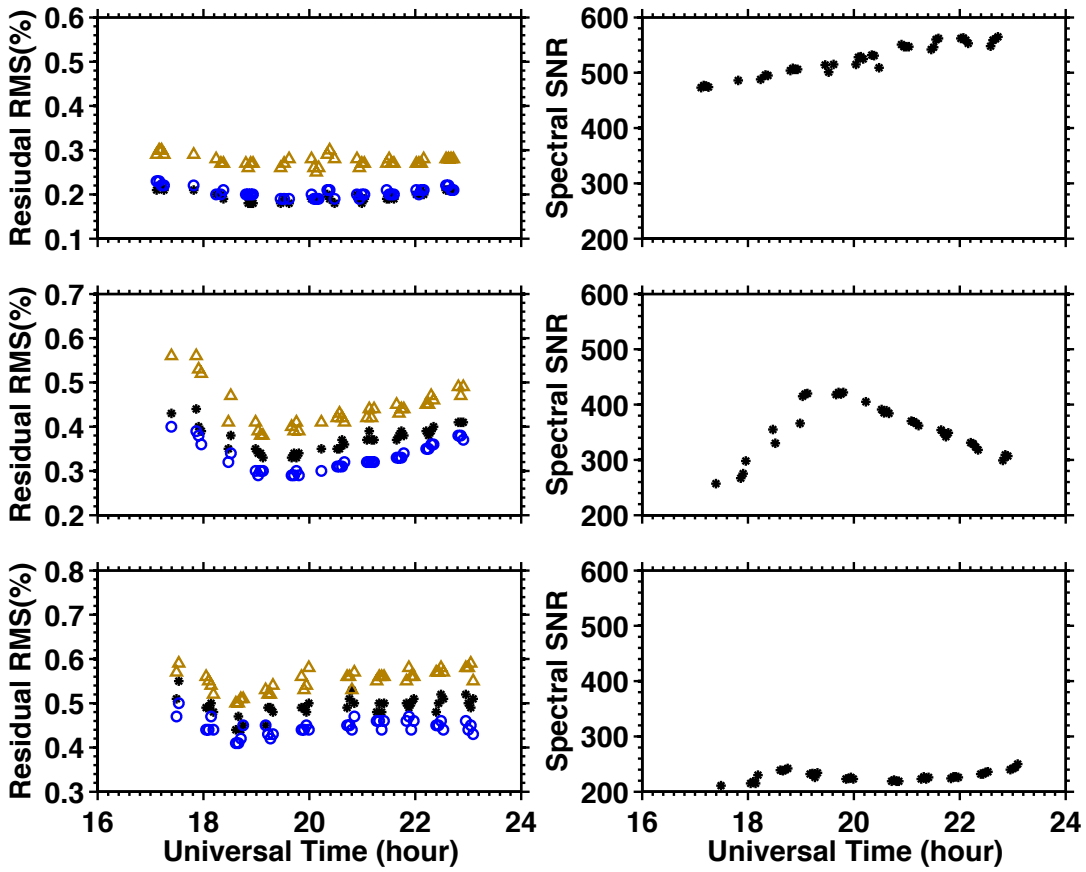

Supplemental Material Figure 9. Root Mean Square (RMS) of spectral fitting residuals (left panels) and spectral SNR (right panels) as a function of time for the measurements of CH_4 and O_2 column densities in Spectralon® viewing geometry (top panels); over the Arcadia Race Track (middle panels); over west Pasadena (bottom panels). Three spectral bands centered at 5938 cm^{-1} (black stars, noted as MW5938 thereafter), 6076 cm^{-1} (blue circles, noted as MW6076 thereafter) and 7885 cm^{-1} (gold triangles, noted as MW7885 thereafter) are presented, respectively. The spectral SNR were nearly identical over the three spectral bands within a measured spectrum, but varies among spectra. The measurements were performed on January 18th, 2013. The spectral fitting residuals were normalized by the spectral continuum levels prior to the computation of RMS values. The spectral fitting residuals were dominated by the photon shot noise since the RMS of the spectral fitting residuals in both CH_4 bands are reasonably close to the expected values, i.e., 1/(spectral SNR). The Chi-squared tests of spectral fitting residuals yielded values generally within 1.3.

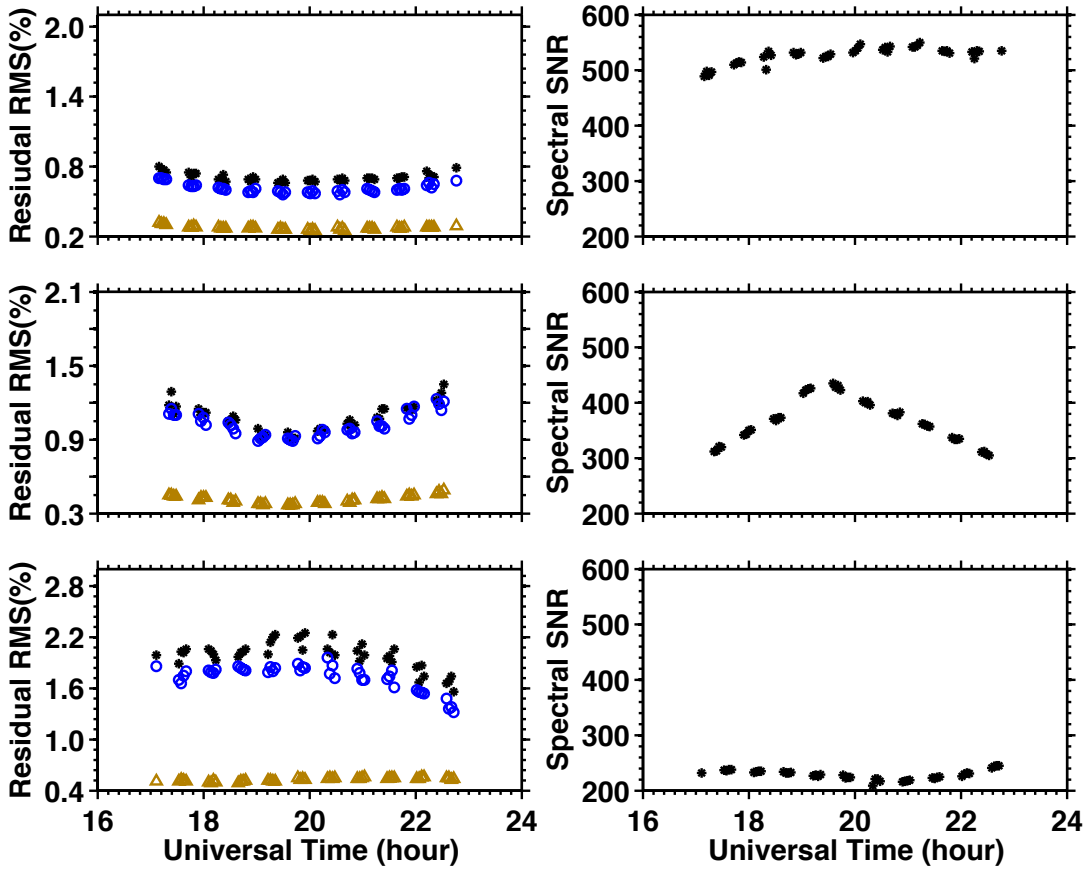

Supplemental Material Figure 10. Root Mean Square (RMS) of spectral fitting residuals (left panels) and spectral SNR (right panels) as a function of time for the measurements of CO and O_2 column densities in Spectralon® viewing geometry (top panels); over the Arcadia Race Track (middle panels); over west Pasadena (bottom panels). Three spectral regions near 2.36 µm centered at 4233 cm^{-1} (black stars, noted as MW4233 thereafter), 4290 cm^{-1} (blue circles, noted as MW4290 thereafter) and O_2 band near 1.2 µm centered at 7885 cm^{-1} (gold triangles, noted as MW7885 thereafter) are presented, respectively. The spectral SNR were nearly identical over the three spectral bands within a measured spectrum, but varies among spectra. The measurements were performed on January 3rd, 2013. The spectral fitting residuals were normalized by the spectral continuum levels prior to the computation of RMS values. The strong absorption of inferring gases other than CO gas in MW4233 and MW4290 made spectral fitting residuals be larger than that of CO_2 CH_4, and O_2. Previous studies reported similar phenomena.

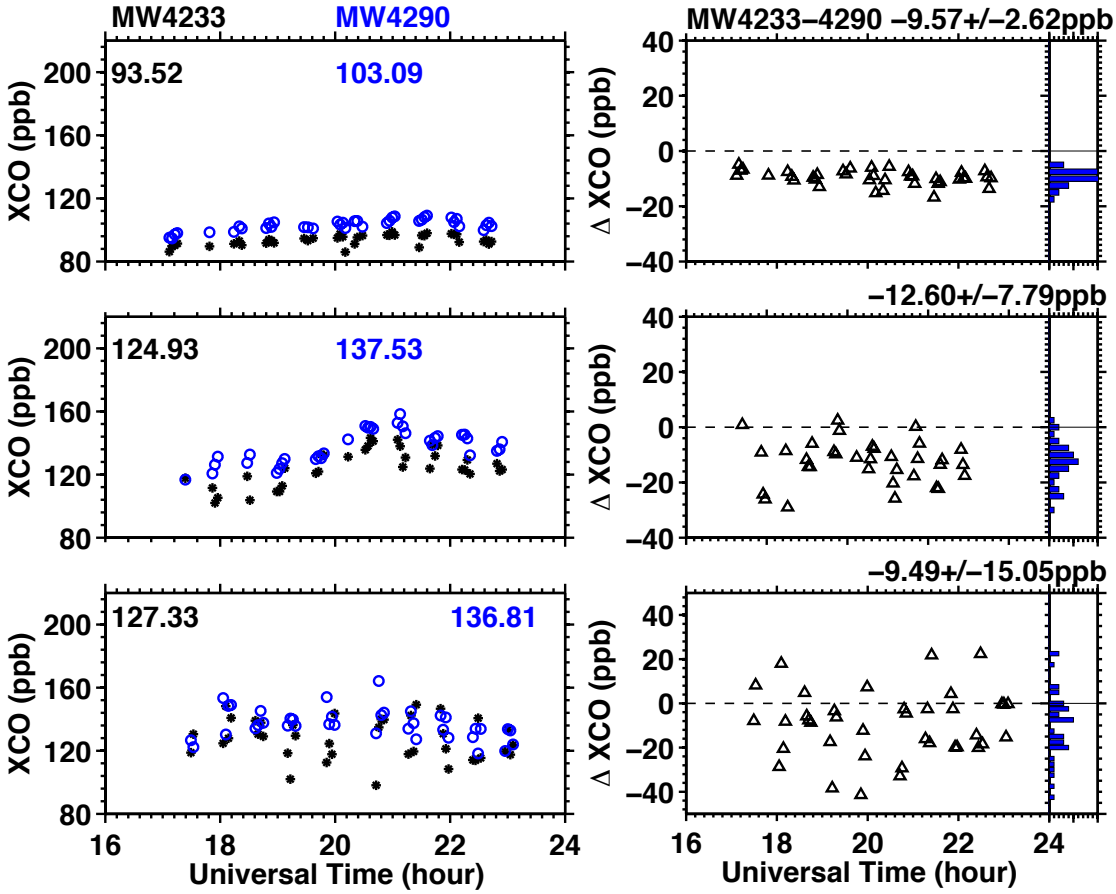

Supplemental Material Figure 11. XCO (in parts per billion (ppb)) measured by CLARS-FTS with MW4233 (black dots) and MW4290 (blue circles) on January 18th, 2013 (left panels) and differences of retrieved XCO between the two spectral regions and the histograms (right panels) in the Spectralon® viewing geometry (top panels), towards the Arcadia Race Track (middle panels); and towards west Pasadena (bottom panels). Compared to the background levels of XCO (top panels), XCO over Arcadia Race Track (middle panels) and west Pasadena (bottom panels) show higher values (mean ART-SV: 32.93 ppb; mean WP-SV: 33.77 ppb) and present stronger diurnal cycles than those measurements over CLARS site. The XCO values retrieved from MW4290 are higher than those of MW4233. The mean differences between MW4290 and MW4233 are 9.57 ppb, 12.60 ppb, and 9.49 ppb for SV, ART and WP respectively. These systematic differences of retrieved XCO values between two spectral bands are likely arisen from the discrepancies of spectroscopic parameters between two spectral bands and the amount/intensity of spectral features of interfering species.